

# GoalNet: Goal Areas Oriented Pedestrian Trajectory Prediction

Ching-Lin Lee, Zhi-Xuan Wang, Kuan-Ting Lai, Amar Fadillah  
National Taipei University of Technology

## Abstract

Predicting the future trajectories of pedestrians on the road is an important task for autonomous driving. The pedestrian trajectory prediction is affected by scene paths, pedestrian's intentions and decision-making, which is a multi-modal problem. Most recent studies use past trajectories to predict a variety of potential future trajectory distributions, which do not account for the scene context and pedestrian targets. Instead of predicting the future trajectory directly, we propose to use scene context and observed trajectory to predict the goal points first, and then reuse the goal points to predict the future trajectories. By leveraging the information from scene context and observed trajectory, the uncertainty can be limited to a few target areas, which represent the "goals" of the pedestrians. In this paper, we propose GoalNet, a new trajectory prediction neural network based on the goal areas of a pedestrian. Our network can predict both pedestrian's trajectories and bounding boxes. The overall model is efficient and modular, and its outputs can be changed according to the usage scenario. Experimental results show that GoalNet significantly improves the previous state-of-the-art performance by 48.7% on the JAAD and 40.8% on the PIE dataset.

## 1. Introduction

Autonomous driving is under rapid technological development and changes in recent years, and the first priority must be safety. In order to achieve this goal, one of the fundamental tasks is to predict the trajectories of pedestrians, which can help autonomous vehicles to avoid collisions in advance. For example, if we cannot predict that a pedestrian is about to cross the road, the vehicle can only start braking when the pedestrian appears in front of it. The short response time may cause failure to stop in time, resulting in casualties. Therefore, estimating pedestrian trajectories quickly and accurately is a crucial task. But trajectory prediction is not an easy task, after all, people's actions and thoughts are constantly changing. There are two main factors that affect the choice of trajectory path. The first factor

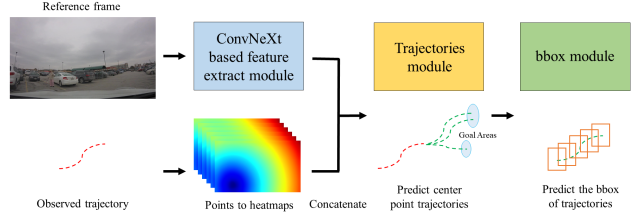


Figure 1. Overview of GoalNet. We use both scene context and observed trajectory to predict goal areas, and then use the goal information to predict pedestrian's trajectories and bounding boxes.

is the pedestrian's past trajectory, which contains the implicit intention. The second factor is the surrounding environment, including passable areas and inaccessible areas. A good pedestrian trajectory prediction model needs to consider these two factors.

Most of the previous trajectory prediction approach were based on the bird's eye view (BEV) datasets (e.g., ETH [27], UCY [20], Stanford Drone Dataset (SDD) [30]). Because the pedestrian trajectory is predicted on the BEV, the 3-dimensional space task is transformed to 2-dimensional, and the fixed viewing angle indicates no self-motion, which simplifies the prediction problems in autonomous driving. In the autonomous driving system or the emergency braking system, the basis for judging the action command comes from the picture information from the perspective of the dashboard camera. Therefore, in the trajectory prediction of autonomous driving, the datasets from the perspective of the dashboard camera will be selected for research, such as JAAD [29] and PIE [28] datasets.

The trajectory prediction part is usually regarded as a problem of time series analysis, so in the early processing of this problem, only the historical trajectory is used as input. However, if it is necessary to further consider the input of scene context at the same time, the two inputs of trajectory and environment need to be converted into the same dimension in the model, and the input of environment is a two-dimensional picture. Since the scene image is 2-dimensional, and the trajectory is 1-dimensional in the original data if the scene image is converted into the

1-dimensional alignment with the trajectory dimension, the spatial information will be lost, but if the trajectory is converted into the 2-dimensional heat map to align with the scene image, this problem can be solved.

In terms of trajectory prediction output, deterministic trajectory prediction was mostly carried out in the early days, while multi-modal trajectory prediction is the mainstream of current trajectory prediction research, that is, multi-modal prediction. Because the pedestrian will change the route of the next action due to different environmental conditions or his ideas at each time step, predicting multiple uncertain trajectories can better represent pedestrian's future trajectory. Studies in [2, 5, 18, 32] also show that multi-modal trajectory prediction is more accurate than deterministic trajectory prediction, and SGNet [34] has also achieved remarkable achievements in uncertainty prediction.

Unlike the regression problem, which treats trajectories directly as sequential patterns, some previous studies, such as Y-Net [25], proposed to address the problem in a novel way. The authors believe that pedestrian trajectory prediction is different from normal linear trajectory because the decision-making subject of trajectory is human, and it is obviously different from general time series forecasting because there are more potential variables of uncertainty in decision-making. The authors of Y-Net mentioned that such uncertain decision factors would have a greater impact on long-term trajectory prediction, and propose a long-term trajectory prediction network with good performance. Our work is inspired by Y-Net, but different from Y-Net's fixed BEV perspective. In our work, we make trajectory prediction based on vehicle FPV perspective, which indicates that the decision variables of the trajectory besides the pedestrians, the driver's decision will have a similar impact on the future movement of the trajectory. And the speed of the vehicle will make these potential decision factors further amplified. Therefore, due to the more complex environmental conditions and the influence of more uncertain factors, the uncertainty trajectory prediction has become more important in our work.

The contributions of this work are summarized as follows: First, we develop a new multi-modal trajectory prediction model GoalNet and show that it has a significant improvement in multi-modal trajectory prediction performance on JAAD and PIE trajectory prediction datasets. Second, different from the conditional variational autoencoder (CVAE) or RNN-based models in the field of trajectory prediction, we apply and integrate many advanced and new convolutional structures and methods. A well-performing design based on convolutional neural networks is proposed for trajectory prediction, and the influence of each sub-network in GoalNet has been studied. Finally, we provide a method to predict the corresponding bounding box trajectory from the center point trajectory. Figure 1

shows the overview structure of GoalNet.

## 2. Related Work

Nowadays, in the field of autonomous driving, the datasets used can mainly divided into two types. One is the datasets containing LiDAR data, such as nuScenes [4] or Argoverse [6]. After using LiDAR data, the dataset can be divided into two types. The ability to 3D detect and track the detected object and to measure its velocity and acceleration makes it possible to increase the accuracy of training autonomous driving-related neural networks by adding effective auxiliary information. In this dataset, some recent studies such as ViP3D [11] have achieved remarkable results. The other is a dataset with only camera images, such as JAAD and PIE, which are cheaper, smaller, and easier to install on vehicles than LiDAR. Especially in recent years, most vehicles have installed dashboard cameras. This means that the trajectory prediction model designed based on the scenarios of such datasets has a broader and universal application prospect. Moreover, the neural network does not need to process the LiDAR data, the memory resources used are less and the execution speed is more advantageous. For most vehicle safety assistance systems with limited hardware resources, these are the characteristics of such embedded systems with extremely limited computing resources.

Early trajectory prediction was mostly studied in fixed-angle bird's eye view, but in BEV the 3D spatial task is simplified to 2D, and the fixed-angle means no self-motion, which simplifies the problem, however, to use it in autonomous driving, it is aided by the traffic recorder image, so recent research has also developed towards the first person view, and our GoalNet also uses FPV dataset to validate the model.

**Bird's Eye View (BEV).** Pedestrian trajectory prediction on BEV mainly simplifies the factor of self-motion, and does the trajectory prediction under the situation of fixed viewing angle and position, and the common datasets are ETH/UCY and SDD. In ETH/UCY, the Y-Net [25] proposed by Mangalam et al. contains RGB scenes and historical trajectories as inputs, semantic segmentation of the scenes and estimation of trajectory endpoint locations and the probability distribution of the path points in them are used for trajectory prediction; The  $V^2$ -Net [35] proposed by Wong et al. adds Fourier transformations to model and predict the trajectories in the spectral trajectory view, a kind of Transformer-based network containing coarse-level key-points estimation and fine-level spectrum interpolation, this has led to an emphasis on pedestrian socialization and interaction with the scene; The NSP-SFM [39] proposed by Yue et al. uses a deterministic model based on microscopic equations, and the key parameters can be learned from the

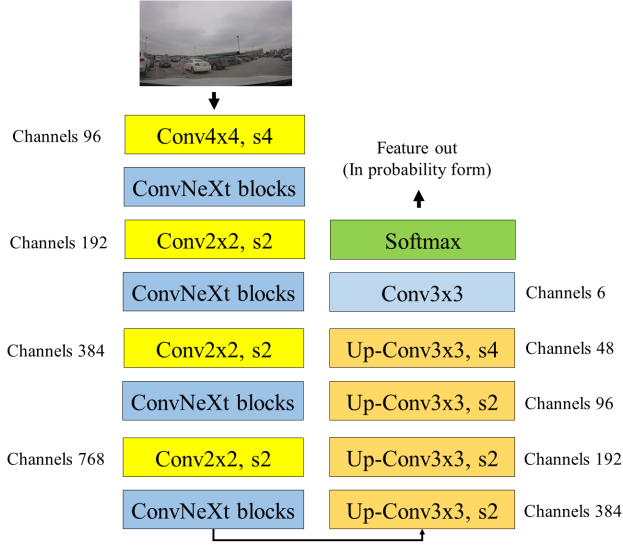


Figure 2. **GoalNet feature extract module architecture.** It consists of a ConvNeXt-T based encoder and a lightweight decoder based on Upsample convolution.

data and integrated into the NSP model using an autoencoder that captures the kinematic dynamics and uncertainty. Trajectory prediction in a top-down view such as the Stanford Drone Dataset has also yielded better results in the  $V^2$ -Net model and NSP-SFM mentioned above. In addition, the TDOR [12] proposed by Guo et al. establishes the CVAE by taking the future trajectories in the neighboring grids as interpretable potential variables. They are iterated in maximum-entropy inverse reinforcement learning through differentiable value iteration networks and to maximize the data possibilities for learning path planning and trajectory generation.

**First Person View (FPV).** Pedestrian trajectory prediction with a first person perspective is more suitable for training automated driving systems, because it includes the vehicle’s self-motion, in which JAAD and PIE datasets are more widely used, and we also used these two datasets for the validation. In 2019 the PIE dataset was released by Rasouli et al. They also proposed an intention estimation and trajectory prediction model with a large number of LSTM modules [28], which achieved good results not only on its own dataset but also on JAAD. Yao et al. proposed the Bitrap model [38], this trajectory prediction model consists of four parts: the condition prior network, the identification network, the target generation network and the trajectory generation network, and uses a large number of GRU modules in the model. It is a multi-modal trajectory pre-

diction model that uses bounding boxes or trajectories as inputs and outputs multiple predicted trajectories. Recently Wang et al. indicated that human intention is a manifestation of planning, and intention at previous time points also changes their view in the present, and proposed SGNet [34], which combines past goals into an encoder through average pooling, and uses an attention mechanism to learn the importance of each goal to the prediction. And both Bitrap and SGNet perform well on JAAD and PIE dataset.

### 3. Proposed Method

The problem of trajectory prediction can be defined as follows. Suppose that the current time is  $t$ , and  $\mathbf{P}$  represents the bounding box coordinates of the object with length and width (in pixels), then  $\mathbf{P}_t$  represents the position of the object at time  $t$ . The given observation time is 15 frames,  $\mathbf{X} = \{\mathbf{P}_{t-14}, \mathbf{P}_{t-13}, \dots, \mathbf{P}_t\}$ , our goal is to predict the position of  $\mathbf{X}$  in the next 45 frames,  $\mathbf{Y} = \{\mathbf{P}_{t+1}, \mathbf{P}_{t+2}, \dots, \mathbf{P}_{t+45}\}$ . For the prediction of stochastic trajectories, given an observation trajectory  $\mathbf{X}$ , there may be multiple results, so various trajectories corresponding to these uncertain futures need to be generated to cover this uncertainty, the uncertain trajectories are expressed as  $\mathbf{S}$ , and the corresponding  $n$  trajectories are generated.  $\mathbf{S} = \{\mathbf{S}_1, \mathbf{S}_2, \dots, \mathbf{S}_n\}$ .

GoalNet consists of three modules, which are feature extraction, trajectory prediction, and bounding box prediction module, and we estimate the number of parameters and FLOPs of our model as shown in Table 1.

modules	#param.	FLOPs
GoalNet - extract	31.347M	22.770G
GoalNet - trajectory	2.131M	20.821G
GoalNet - bbox	0.174M	0.174M
Total	33.652M	43.591G

Table 1. GoalNet #param. & FLOPs.

#### 3.1. Feature Extract Module

Scene context is very important for trajectory prediction, but many previous studies [1, 13, 34, 38] only deal with trajectory without considering environmental images. On specific trajectory datasets (e.g., Stanford Drone Dataset (SDD) [30]), some studies [21, 22] begin to use segmentation as an environmental feature extraction method. However, for most trajectory prediction datasets, In particular, it is not an easy task to construct segmentation annotation for first person perspective (FPV) datasets, and it is difficult to define appropriate classes, and the output channels are not very flexible, because they depend on the number of segmentation classes. If RGB scene images are directly input into the trajectory prediction model, the trajectory predic-

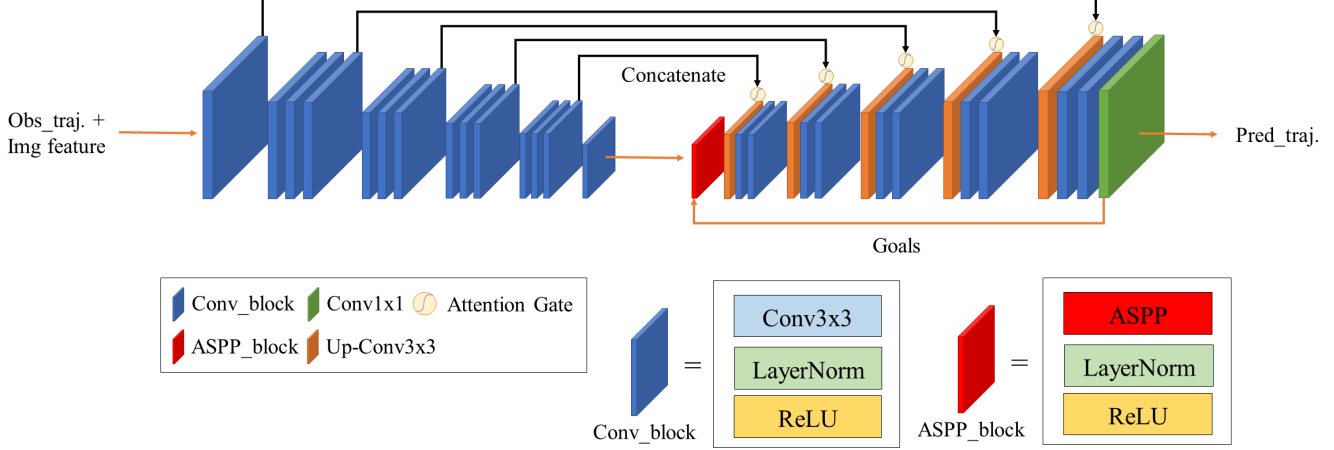


Figure 3. Trajectory module designs for GoalNet.

tion model needs to adapt to the processing of environmental images and trajectory information at the same time. In order to make the trajectory prediction model consider both scene context and trajectory information, the trajectory prediction module focuses on trajectory coding. Rather than directly input RGB images into the trajectory prediction model, it is necessary to establish the image and maintain the hidden state of complete spatial information through feature extraction. Indirectly inputting the scene image into the trajectory prediction module is a better method.

We implemented the feature extraction module based on ConvNeXt [23], the structure of which is shown in Figure 2. Considering the computational load of this module and the trajectory prediction module, we chose the smallest ConvNeXt-Tiny as the encoder. After extracting the feature map through ConvNeXt-Tiny, the decoder uses the same but greatly simplified steps as downsample to upsample back the feature map to the size of the original RGB image and normalizes the features to probability distribution through softmax, because softmax can enlarge the feature differences. Highlight important feature areas within each channel.

### 3.2. Trajectory Module

In the trajectory prediction module, the same two-dimensional processing method as the environmental image can avoid the loss of spatial information contained in the environmental image. Some previous studies [8,33,37] mostly adopted the RNN-based trajectory prediction model. However, when the environmental image is encoded as a one-dimensional hidden state, the spatial information contained in the environmental image will be completely destroyed. Therefore, we converted the trajectory to the heatmap form to transform the trajectory into a two-dimensional space representation aligned with the representation of the scene

image.

This module encodes the observed trajectory and the scene image, and the decoder predicts the goal areas represented by a probability distribution, and calculates the main goal through spatial soft arg-max [9]. At the same time, K-means clustering algorithm is used to calculate the secondary goals in the goal areas, and these goals are input back to the decoder in sequence again to generate uncertainty trajectories with these goals as future assumptions.

As a classic convolutional encoder-decoder network structure, U-Net [31] was originally designed for segmentation. Still, the trajectory is highly correlated with space, so designing a structure similar to U-Net is potentially beneficial. Y-Net [25] has proven this.

Batch Normalization (BN) [17] was used in the U-Net, but BN of trajectories will corrupt the information. So BN should be replaced with a batch independent normalization method, like Group normalization (GN) [36] or Layer Normalization (LN) [3]. The GN restriction that channels must be divisible by the group severely limits model design, the combination of LN and Atrous Spatial Pyramid Pooling (ASPP) [7] matches better. So we chose to use LN to substitute the BN.

Since trajectory prediction does not require a special ability to perceive the edge of an object like segmentation, stride 2 convolution, like modern convolutional networks such as ResNet [15] and ConvNeXt [23] is probably more advantageous in this case. Therefore, we replace the U-Net downsample method with stride 2 convolution. At the same time, by replacing the convolution layer with ASPP at the deepest (Center layer) of the trajectory prediction module, the perception field of view of the model is greatly improved, and the spatial information of the trajectory is more fully utilized.

In addition, the Attention Gate (AG) technique is pro-

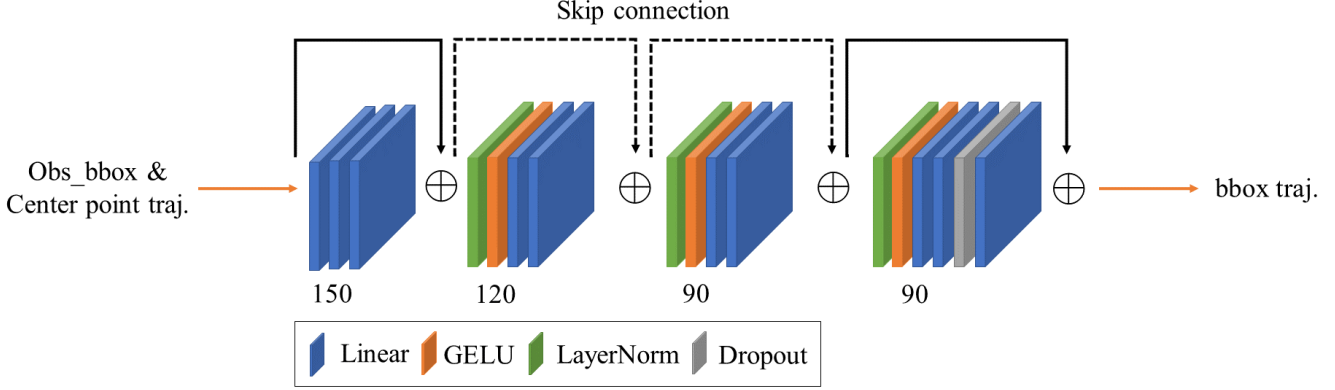


Figure 4. **bbox module architecture of GoalNet.** Solid line indicates that the skip connection is a direct connection. Dashed lines indicate that the number of channels in the skip connection has been converted.

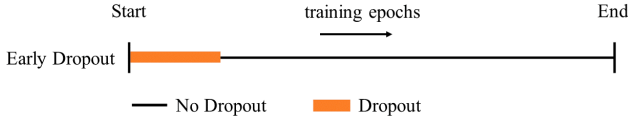


Figure 5. **Early Dropout.** This method improves the generalization and final accuracy of the model.

posed in attention U-Net [26], and it has been proved that AG can enhance attention to important regions in feature maps concatenated by the encoder. Since our trajectory prediction module is similar to U-Net and AG is not designed for segmentation, but belongs to a more general technology, we add AG to our trajectory prediction module. The final trajectory prediction module structure is shown in Figure 3.

### 3.3. Bounding Box Module

In Figure 4, in order to predict the bounding box corresponding to the trajectory, we convert the center point trajectory predicted by the trajectory prediction module to the trajectory in the form of bounding box by predicting the width and height of the bounding box. Different from previous studies [34, 38], previous studies directly predicted bounding box location, coordinates sequences representing the upper left and lower right points of bounding box, and then calculated the trajectory of its center point. In our work, it is not easy to generate two points at a time in a single time step, so we adopt the opposite method, that is, first predict the location, coordinates of the center point, and then predict the trajectory in the form of bounding box. As shown in the table 1, the computational consumption of this method can be almost ignored.

This module uses the fully connected layer design, and PreAct ResNet [16] proves that it is more beneficial to reduce the layers on skip connection that hinder the propaga-

tion of gradient flow, so the residual structure in our module is designed in a similar way to PreAct. In addition, recent studies have shown that the final accuracy of the model can be improved by using Early-Dropout [24], so we adopted this method (Figure 5).

### 3.4. Loss Functions

Since the predicted trajectory is the probability distribution of each timestep, and the feature extraction module does not make an actual prediction, but only generates environmental features for the trajectory prediction module. Therefore, we use binary cross-entropy loss to supervise the prediction of trajectory feature extraction and prediction module. For the bounding box prediction module, since the prediction results are absolute values of width and height, we use SmoothL1Loss [10] to monitor. Thus, for each training sample, our final loss is summarized as follows,

$$\mathcal{L}_{traj} = BCEWithLogits(P(\mathbf{Y}), P(\mathbf{Y}_{gt})), \quad (1)$$

$$\mathcal{L}_{bbox} = SmoothL1(\mathbf{Y}_{wh}, \mathbf{Y}_{wh-gt}), \quad (2)$$

$$\mathcal{L}_{total} = \mathcal{L}_{traj} + \mathcal{L}_{bbox}, \quad (3)$$

Where,  $P(\mathbf{Y})$  is the probability distribution of the predicted trajectory at each timestep in the future, and  $P(\mathbf{Y}_{gt})$  is the heatmap transformed by the ground truth coordinate of the target object in the future.  $\mathbf{Y}_{wh}$  is the width and height of the predicted trajectory bounding box at each point in time in the future, and  $\mathbf{Y}_{wh-gt}$  is the true size of the target object in the future.

## 4. Experiments

In this section, we use a total of two publicly available trajectory prediction datasets on pedestrian behavior in traffic to study the performance of GoalNet.



Method (Best of 20)	JAAD				PIE			
	MSE↓	CMSE↓	CFMSE↓	NLL↓	MSE↓	CMSE↓	CFMSE↓	NLL↓
	(0.5s / 1.0s / 1.5s)	(1.5s)	(1.5s)		(0.5s / 1.0s / 1.5s)	(1.5s)	(1.5s)	
BiTraP-GMM [38]	153 / 250 / 585	501	998	<b>16.0</b>	38 / 90 / 209	171	368	<b>13.8</b>
BiTraP-NP [38]	38 / 94 / 222	177	565	18.9	23 / 48 / 102	81	261	16.5
SGNet-ED [34]	37 / 86 / 197	146	443	-	16 / 39 / 88	66	206	-
ABC+ [14]	40 / 89 / 189	145	409	-	16 / 38 / 87	65	191	-
GoalNet	<b>31 / 67 / 133</b>	<b>97</b>	<b>215</b>	17.8	<b>15 / 32 / 65</b>	<b>44</b>	<b>97</b>	15.7

Table 2. Stochastic results ( $K=20$ ) on JAAD and PIE in terms of MSE/CMSE/CFMSE. ↓ denotes lower is better.

Case	MSE↓ (0.5s / 1.0s / 1.5s)	CMSE↓ (1.5s)	CFMSE↓ (1.5s)
w/o feature extract module	34 / 72 / 144	108	272
w/o Attention-Gate	33 / 72 / 139	103	229
w/o ASPP	30 / 69 / 137	100	235
GoalNet	<b>31 / 67 / 133</b>	<b>97</b>	<b>215</b>

(a) Macro design.

Case	MSE↓ (0.5s / 1.0s / 1.5s)	CMSE↓ (1.5s)	CFMSE↓ (1.5s)
ReLU	<b>31 / 67 / 133</b>	<b>97</b>	<b>215</b>
Leaky ReLU(0.1)	31 / 69 / 137	101	216
PReLU	30 / 65 / 134	98	233
SiLU	33 / 72 / 141	104	222
GELU	32 / 72 / 149	111	267

(c) Activation function. ReLU is simple and efficient.

Case	MSE↓ (0.5s / 1.0s / 1.5s)	CMSE↓ (1.5s)	CFMSE↓ (1.5s)
w/o norm.	30 / 67 / 136	100	249
BN	114 / 235 / 446	403	1028
GN	32 / 70 / 141	104	232
LN	<b>31 / 67 / 133</b>	<b>97</b>	<b>215</b>

(b) Feature normalization. LayerNorm outperforms other normalizations.

Case	MSE↓ (0.5s / 1.0s / 1.5s)	CMSE↓ (1.5s)	CFMSE↓ (1.5s)
Conv (stride 2)	<b>31 / 67 / 133</b>	<b>97</b>	<b>215</b>
MaxPool	30 / 67 / 134	97	221
AvgPool	30 / 66 / 136	98	240

(d) Feature downsample.

Table 3. Exploration study of our model on JAAD. ↓ denotes lower is better. Our final proposal is marked in gray.

**Datasets.** Joint Attention in Autonomous Driving (JAAD) [29] and Pedestrian Intention Estimation (PIE) [28] Dataset are used in our experiment. Trajectories for both datasets were recorded using an on-board camera, recorded and annotated at 30 frames per second (FPS). JAAD contained 2,800 pedestrian trajectories out of 75,000 annotated frames, while PIE contained 1,800 pedestrian trajectories out of 293,000 annotated frames, with longer annotated trajectories and more comprehensive annotations than JAAD. We followed the JAAD and PIE standard training/testing split [28], using the same observation and prediction lengths as prior work [34, 38]. A trajectory with a length of 0.5 seconds (15 frames) is input to generate a trajectory with a length of 0.5, 1.0, 1.5 seconds (15, 30, 45 frames).

**Implementation Details.** We use ConvNeXt-Tiny [23] as the backbone of the feature extraction module, convert the two-dimensional input of RGB 3 channels into two-dimensional output of 6 channels, and implement the encoder-decoder of the trajectory prediction module using a U-Net-like structure. The input of the trajectory prediction module is taken by the observed 15-time step trajectory heatmap as 15 channels and concatenate with 6 channels scene feature map. The channel size of the encoder is 32-

32-64-64-64-128, while the decoder is the opposite, and the trajectory prediction output of 45 time steps is generated. The last point of the first output trajectory is feedback to the decoder as a goal to generate the final future trajectories. All models were trained with a batch size of 8, the Adam [19] optimizer with an initial learning rate of 1e-4, and the ReduceLROnPlateau scheduler on a single RTX2080Ti GPU.

**Evaluation Metrics.** Following [28, 29, 34, 38], our GoalNet model uses Mean Square Error (MSE), Center Mean Square Error (CMSE), Center Final Mean Square Error (CFMSE) and Kernel Density Estimation-based Negative Log Likelihood (KDE-NLL) to evaluate our performance on JAAD and PIE in pixels. MSE is calculated according to the upper left and lower right coordinates of the bounding box trajectory. CMSE and CFMSE are calculated using the center point of the bounding box trajectory. Calculate the NLL of the ground truth under a probability distribution fitted by KDE using 2000 trajectory samples.

#### 4.1. Experiments on JAAD and PIE datasets

We compared the results with the following baseline models: 1) BiTraP-GMM 2) BiTraP-NP 3) SGNet-ED. To make a fair comparison of stochastic results with [34, 38]

in JAAD and PIE Benchmarks, we generate  $K = 20$  proposals and report the best sample. Table 2 shows the trajectory prediction results of JAAD and PIE datasets. The results show that our method significantly outperforms previous state-of-the-art methods by an average of 48.7% on JAAD and 40.8% on PIE.

Although the NLL metrics is not the best, the reason is that the multi-modal trajectory distribution generated by BiTraP-GMM is similar to ground truth, but each trajectory has a high displacement error. Our method has lower displacement error and better multi-modal trajectory distribution than BiTraP-NP.

## 4.2. Exploration Study

To design our GoalNet model and make predictions on the JAAD and PIE datasets, we use the U-Net [31] architecture as a base, and reference modern convolutional neural network designs such as ConvNeXt [23]. Evaluate the sub-modules and micro-designs of the overall GoalNet design, the result is shown in Table 3.

Table 3a analyzes the impact of removing different modules on GoalNet. The results show that the feature extraction module is necessary. If the environment RGB image is directly input into the trajectory prediction module, the final accuracy will be greatly reduced. And removing either the

Attention Gate (AG) [26] or Atrous Spatial Pyramid Pooling (ASPP) [7] modules would result in lower final accuracy, so adding AG and ASPP does have a positive effect on the model.

Table 3b analyzes the performance using different normalization layers, and while Batch Normalization (BN) [17] is an important and common component in convolutional neural networks and is preferred for many visual tasks, because it improves the convergence of the model and reduces overfitting, but experiments show that BN is very unsuitable for use in our structure, and the experimental data show that Group Normalization (GN) [36] is better than BN. However, the implementation of layer normalization of GN is very similar to BN, the difference is that GN avoids some of the batch restrictions of BN by group normalization of channels within a single training sample, and we speculate that normalization on batches will destroy some important information in the training data. In recent years, Layer Normalization (LN) [3] has gradually increased in importance and replaced BN gradually, including replacing BN with LN in transformer and ConvNeXt. ConvNeXt shows that it is not difficult to replace BN with LN in convolutional neural networks, and it is possible to achieve better results. Our experiments also show that LN does perform best, so LN is used as the layer normalization choice in our model.



Figure 6. **JAAD Qualitative Results.** The cyan color indicates the observed trajectory, the red color indicates the ground truth future trajectory, and the green color indicates the predictions from our GoalNet model.

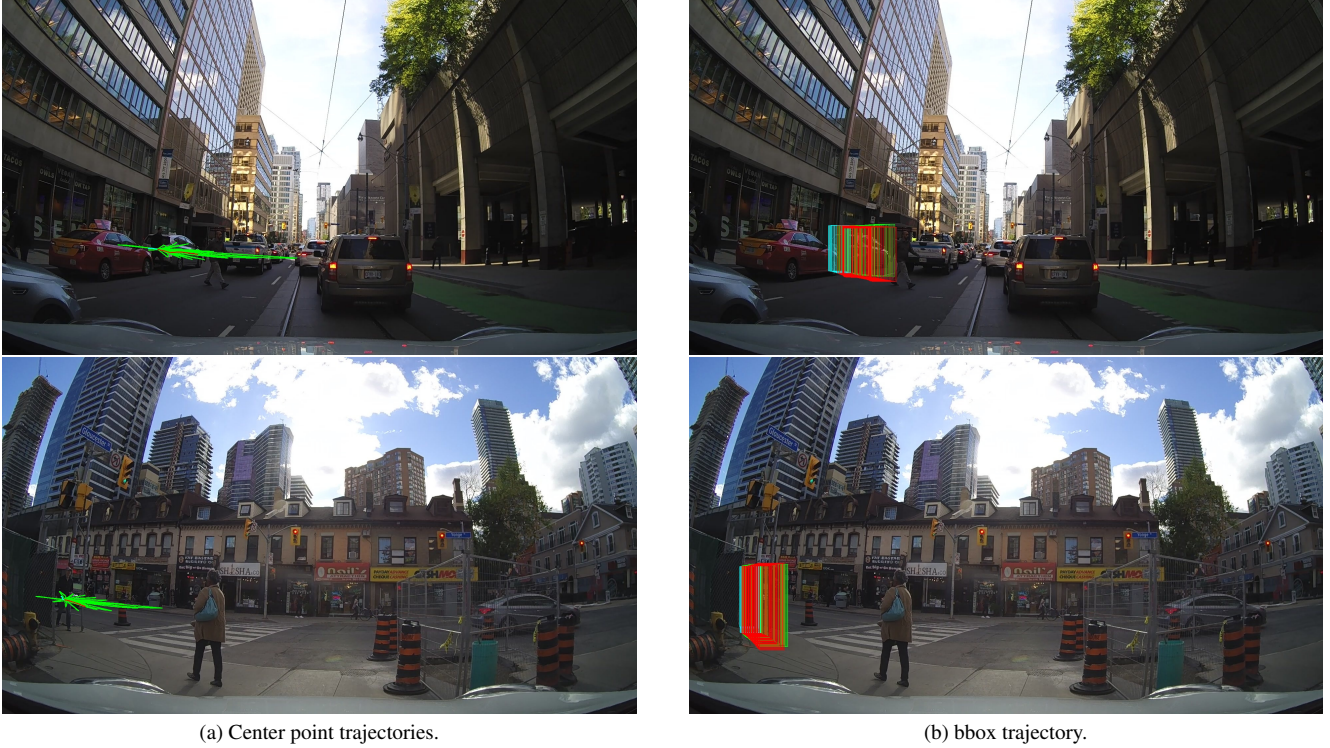


Figure 7. **PIE Qualitative Results.** The cyan color indicates the observed trajectory, the red color indicates the ground truth future trajectory, and the green color indicates the predictions from our GoalNet model.

The results of different activation functions are discussed in Table 3c. Rectified Linear Unit (ReLU) is widely used in convolutional neural networks, and due to the dying ReLU problem, ReLU has therefore derived many variants (e.g., LeakyReLU, PReLU, GELU) to solve this problem. Experiments have shown that ReLU performs best in our model, so we have chosen to continue using ReLU in our model.

The influence of different downsampling layers is studied in Table 3d. Max Pooling is often used in previous networks, it retains key features by taking the maximum value during downsampling. In addition, Max Pooling’s gradient flow propagation is easier than stride 2 convolution, which makes it easier for neural networks to learn. However, in modern convolutional neural networks, stride 2 convolution is often used to replace Pooling, because stride 2 convolution has learnable parameters. With appropriate design, some accuracy advantages may be achieved.

### 4.3. Qualitative Results

Figure 6 and Figure 7 show GoalNet’s prediction results on the test split of the JAAD and PIE datasets, respectively. (a) Show the prediction results for all 20 uncertain trajectories. Most of the multi-modal prediction results are close to the ground truth trajectory in the future, and the high

probability distribution near the ground truth trajectory is successfully predicted, which also indicates the stability of the model and converges the uncertainty to a certain range. (b) The best bounding box trajectory is shown. The results show that our model can correctly predict the scaling of the bounding box as the pedestrian approaches or moves away from the vehicle.

The predicted future trajectory in the scene not only shows the trajectory and intention of the pedestrian, but also includes the movement of the vehicle itself. The predicted result also represents the relative position of the pedestrian and vehicle after the specified time step. For the vehicle assistance system, the relative position of the pedestrian and the vehicle in the future is obviously helpful to the safety decision of the system.

## 5. Conclusion

We propose a multi-modal uncertainty trajectory prediction model called GoalNet based on convolutional neural networks. It is also demonstrated that our proposed model can achieve state-of-the-art results on first-person datasets suitable for autonomous driving training. Overall, GoalNet improved previous state-of-art performance on JAAD by 48.7% and improved it by 40.8% on PIE. For future work, we expect to further expand our model with optional



modular modules such as social collisions, intentions, LiDAR, etc., so that the model can flexibly make predictions based on the information it has to further ensure universality while making the best use of available information to improve safety.

## References

- [1] Alexandre Alahi, Kratarth Goel, Vignesh Ramanathan, Alexandre Robicquet, Li Fei-Fei, and Silvio Savarese. Social lstm: Human trajectory prediction in crowded spaces. In *Proceedings of the IEEE/CVF Conference on Computer Vision and Pattern Recognition (CVPR)*, pages 961–971, 2016. [3](#)
- [2] Cyrus Anderson, Xiaoxiao Du, Ram Vasudevan, and Matthew Johnson-Roberson. Stochastic sampling simulation for pedestrian trajectory prediction. In *Proceedings of the IEEE/RSJ International Conference on Intelligent Robots and Systems (IROS)*, pages 4236–4243, 2019. [2](#)
- [3] Jimmy Lei Ba, Jamie Ryan Kiros, and Geoffrey E Hinton. Layer normalization. *arXiv preprint arXiv:1607.06450*, 2016. [4](#), [7](#)
- [4] Holger Caesar, Varun Bankiti, Alex H Lang, Sourabh Vora, Venice Erin Liong, Qiang Xu, Anush Krishnan, Yu Pan, Giancarlo Baldan, and Oscar Beijbom. nuscenes: A multi-modal dataset for autonomous driving. In *Proceedings of the IEEE/CVF Conference on Computer Vision and Pattern Recognition (CVPR)*, pages 11621–11631, 2020. [2](#)
- [5] Yuning Chai, Benjamin Sapp, Mayank Bansal, and Dragomir Anguelov. Multipath: Multiple probabilistic anchor trajectory hypotheses for behavior prediction. In Leslie Pack Kaelbling, Danica Kragic, and Komei Sugiura, editors, *Proceedings of the Conference on Robot Learning (CoRL)*, volume 100 of *Proceedings of Machine Learning Research*, pages 86–99. PMLR, 30 Oct–01 Nov 2020. [2](#)
- [6] Ming-Fang Chang, John Lambert, Patsorn Sangkloy, Jagjeet Singh, Slawomir Bak, Andrew Hartnett, De Wang, Peter Carr, Simon Lucey, Deva Ramanan, et al. Argoverse: 3d tracking and forecasting with rich maps. In *Proceedings of the IEEE/CVF Conference on Computer Vision and Pattern Recognition (CVPR)*, pages 8748–8757, 2019. [2](#)
- [7] Liang-Chieh Chen, George Papandreou, Iasonas Kokkinos, Kevin Murphy, and Alan L Yuille. Deeplab: Semantic image segmentation with deep convolutional nets, atrous convolution, and fully connected crfs. *Proceedings of the IEEE transactions on pattern analysis and machine intelligence*, 40(4):834–848, 2017. [4](#), [7](#)
- [8] Phillip Czech, Markus Braun, Ulrich Kreßel, and Bin Yang. On-board pedestrian trajectory prediction using behavioral features. In *Proceedings of the IEEE International Conference on Machine Learning and Applications (ICMLA)*, pages 437–443, 2022. [4](#)
- [9] Chelsea Finn, Xin Yu Tan, Yan Duan, Trevor Darrell, Sergey Levine, and Pieter Abbeel. Deep spatial autoencoders for visuomotor learning. In *IEEE International Conference on Robotics and Automation (ICRA)*, page 512–519. IEEE Press, 2016. [4](#)
- [10] Ross Girshick. Fast r-cnn. In *Proceedings of the IEEE/CVF International Conference on Computer Vision (ICCV)*, pages 1440–1448, 2015. [5](#)
- [11] Junru Gu, Chenxu Hu, Tianyuan Zhang, Xuanyao Chen, Yilun Wang, Yue Wang, and Hang Zhao. Vip3d: End-to-end visual trajectory prediction via 3d agent queries. In *Proceedings of the IEEE/CVF Conference on Computer Vision and Pattern Recognition (CVPR)*, pages 5496–5506, 2023. [2](#)
- [12] Ke Guo, Wenxi Liu, and Jia Pan. End-to-end trajectory distribution prediction based on occupancy grid maps. In *Proceedings of the IEEE/CVF Conference on Computer Vision and Pattern Recognition (CVPR)*, pages 2242–2251, 2022. [3](#)
- [13] Agrim Gupta, Justin Johnson, Li Fei-Fei, Silvio Savarese, and Alexandre Alahi. Social gan: Socially acceptable trajectories with generative adversarial networks. In *Proceedings of the IEEE/CVF Conference on Computer Vision and Pattern Recognition (CVPR)*, pages 2255–2264, 2018. [3](#)
- [14] Marah Halawa, Olaf Hellwich, and Pia Bideau. Action-based contrastive learning for trajectory prediction. In *Proceedings of the European Conference on Computer Vision (ECCV)*, page 143–159. Springer-Verlag, 2022. [6](#)
- [15] Kaiming He, Xiangyu Zhang, Shaoqing Ren, and Jian Sun. Deep residual learning for image recognition. In *Proceedings of the IEEE/CVF Conference on Computer Vision and Pattern Recognition (CVPR)*, pages 770–778, 2016. [4](#)
- [16] Kaiming He, Xiangyu Zhang, Shaoqing Ren, and Jian Sun. Identity mappings in deep residual networks. In *Proceedings of the European Conference on Computer Vision (ECCV)*, pages 630–645. Springer, 2016. [5](#)
- [17] Sergey Ioffe. Batch renormalization: Towards reducing minibatch dependence in batch-normalized models. *Advances in neural information processing systems*, 30, 2017. [4](#), [7](#)
- [18] Boris Ivanovic and Marco Pavone. The trajectron: Probabilistic multi-agent trajectory modeling with dynamic spatiotemporal graphs. In *Proceedings of the IEEE/CVF International Conference on Computer Vision (ICCV)*, pages 2375–2384, 2019. [2](#)
- [19] Diederik Kingma and Jimmy Ba. Adam: A method for stochastic optimization. In *International Conference on Learning Representations (ICLR)*, San Diego, CA, USA, 2015. [6](#)
- [20] Alon Lerner, Yiorgos Chrysanthou, and Dani Lischinski. Crowds by example. In *Proceedings of the Computer Graphics Forum (CGF)*, pages 655–664. Wiley Online Library, 2007. [1](#)
- [21] Junwei Liang, Lu Jiang, and Alexander Hauptmann. Simaug: Learning robust representations from simulation for trajectory prediction. In *Proceedings of the European Conference on Computer Vision (ECCV)*, page 275–292, Berlin, Heidelberg, 2020. Springer-Verlag. [3](#)
- [22] Junwei Liang, Lu Jiang, Kevin Murphy, Ting Yu, and Alexander Hauptmann. The garden of forking paths: Towards multi-future trajectory prediction. In *Proceedings of the IEEE/CVF Conference on Computer Vision and Pattern Recognition (CVPR)*, pages 10508–10518, 2020. [3](#)
- [23] Zhuang Liu, Hanzi Mao, Chao-Yuan Wu, Christoph Feichtenhof, Trevor Darrell, and Saining Xie. A convnet for the

- 2020s. In *Proceedings of the IEEE/CVF Conference on Computer Vision and Pattern Recognition (CVPR)*, pages 11976–11986, 2022. 4, 6, 7
- [24] Zhuang Liu, Zhiqiu Xu, Joseph Jin, Zhiqiang Shen, and Trevor Darrell. Dropout reduces underfitting. In *Proceedings of the 40th International Conference on Machine Learning (ICML)*. JMLR.org, 2023. 5
- [25] Karttikeya Mangalam, Yang An, Harshayu Girase, and Jitendra Malik. From goals, waypoints & paths to long term human trajectory forecasting. In *Proceedings of the IEEE/CVF International Conference on Computer Vision (ICCV)*, pages 15233–15242, 2021. 2, 4
- [26] Ozan Oktay, Jo Schlemper, Loic Le Folgoc, Matthew Lee, Mattias Heinrich, Kazunari Misawa, Kensaku Mori, Steven McDonagh, Nils Y Hammerla, Bernhard Kainz, Ben Glocker, and Daniel Rueckert. Attention u-net: Learning where to look for the pancreas. In *Medical Imaging with Deep Learning*, 2018. 5, 7
- [27] Stefano Pellegrini, Andreas Ess, and Luc Van Gool. Improving data association by joint modeling of pedestrian trajectories and groupings. In *Proceedings of the European Conference on Computer Vision (ECCV)*, pages 452–465. Springer, 2010. 1
- [28] Amir Rasouli, Iuliia Kotseruba, Toni Kunic, and John K. Tsotsos. Pie: A large-scale dataset and models for pedestrian intention estimation and trajectory prediction. In *Proceedings of the IEEE/CVF International Conference on Computer Vision (ICCV)*, 2019. 1, 3, 6
- [29] Amir Rasouli, Iuliia Kotseruba, and John K Tsotsos. Are they going to cross? a benchmark dataset and baseline for pedestrian crosswalk behavior. In *Proceedings of the IEEE/CVF International Conference on Computer Vision (ICCV)*, pages 206–213, 2017. 1, 6
- [30] Alexandre Robicquet, Amir Sadeghian, Alexandre Alahi, and Silvio Savarese. Learning social etiquette: Human trajectory understanding in crowded scenes. In *Proceedings of the European Conference on Computer Vision (ECCV)*, pages 549–565. Springer, 2016. 1, 3
- [31] Olaf Ronneberger, Philipp Fischer, and Thomas Brox. U-net: Convolutional networks for biomedical image segmentation. In *Proceedings of the Medical Image Computing and Computer Assisted Intervention (MICCAI)*, pages 234–241. Springer, 2015. 4, 7
- [32] Tim Salzmann, Boris Ivanovic, Punarjay Chakravarty, and Marco Pavone. Trajectron++: Dynamically-feasible trajectory forecasting with heterogeneous data. In *Proceedings of the European Conference on Computer Vision (ECCV)*, pages 683–700. Springer, 2020. 2
- [33] Haowen Tang, Ping Wei, Jiapeng Li, and Nanning Zheng. Evostgat: Evolving spatiotemporal graph attention networks for pedestrian trajectory prediction. *Neurocomputing*, 491:333–342, 2022. 4
- [34] Chuhua Wang, Yuchen Wang, Mingze Xu, and David J Crandall. Stepwise goal-driven networks for trajectory prediction. *IEEE Robotics and Automation Letters*, 7(2):2716–2723, 2022. 2, 3, 5, 6
- [35] Conghao Wong, Beihao Xia, Ziming Hong, Qinmu Peng, Wei Yuan, Qiong Cao, Yibo Yang, and Xinge You. View ver-  
tically: A hierarchical network for trajectory prediction via fourier spectrums. In *Proceedings of the European Conference on Computer Vision (ECCV)*, pages 682–700. Springer, 2022. 2
- [36] Yuxin Wu and Kaiming He. Group normalization. In *Proceedings of the European Conference on Computer Vision (ECCV)*, pages 3–19, 2018. 4, 7
- [37] Hao Xue, Du Q Huynh, and Mark Reynolds. Poppl: Pedestrian trajectory prediction by lstm with automatic route class clustering. *IEEE transactions on neural networks and learning systems*, 32(1):77–90, 2020. 4
- [38] Yu Yao, Ella Atkins, Matthew Johnson-Roberson, Ram Vasudevan, and Xiaoxiao Du. Bitrap: Bi-directional pedestrian trajectory prediction with multi-modal goal estimation. *IEEE Robotics and Automation Letters*, 6(2):1463–1470, 2021. 3, 5, 6
- [39] Jiangbei Yue, Dinesh Manocha, and He Wang. Human trajectory prediction via neural social physics. In *Proceedings of the European Conference on Computer Vision (ECCV)*, pages 376–394. Springer, 2022. 2